Estimation of Volumetric Myocardial Apparent Conductivity From Endocardial Electro-Anatomical Mapping

Phani Chinchapatnam, Kawal S. Rhode, Matthew Ginks, Tommaso Mansi, Jean-Marc Peyrat, Pier Lambiase, C. Aldo Rinaldi, Reza Razavi, Simon Arridge and Maxime Sermesant

Abstract— **Estimating patient-specific electrical tissue parameters is of considerable benefit towards personalisation of cardiac biophysical models. In this paper, an adaptive inverse parameter estimation algorithm is proposed to estimate the myocardial apparent conductivity from endocardial electrical potential measurements. The forward electrophysiology problem is posed as an Eikonal model and is solved using an anisotropic fast marching method. The conductivity estimation algorithm is validated on patient data obtained using hybrid X-ray/magnetic resonance imaging. Future directions towards improving such estimation procedures are also indicated.**

I. INTRODUCTION

Cardiac biophysical modelling aims to develop computational models that can simulate realistic human heart motion and function *in silico*. During the last decade, major progress in medical imaging, cardiac modelling and computational power have made personalised simulations achievable. While the scientific importance and enormous clinical potential of the biophysical approach have been acknowledged [1], [2], its translation into clinical applications largely remains to be done. Estimation of patient-specific tissue parameters will largely improve the capabilities of such personalised models and thus facilitate rapid clinical translation. In this paper, we focus on personalisation of cardiac electrophysiology models by estimating an apparent electrical conductivity parameter.

Modelling the cell electrophysiology has been an active area of research since the seminal work of Hodgkin and Huxley [3]. The precise modelling of the myocardium involves a cell membrane model embedded into a set of partial differential equations (PDE) modelling a continuum. We can divide these models into three categories, from the more complex to the more simpler (numerically):

Phani Chinchapatnam (`p.chinchapatnam@cs.ucl.ac.uk`) and Simon Arridge are with the Centre for Medical Image Computing, University College London, Gower Street, London, WC1E 6BT, U.K.

Kawal S. Rhode, Matthew Ginks and Reza Razavi are with the Interdisciplinary Medical Imaging Group, Division of Imaging Sciences, King's College London, 4th Floor Lambeth Wing, St Thomas' Hospital, London, SE1 7EH, U.K.

Tommaso Mansi and Jean-Marc Peyrat are with the Asclepios project, INRIA, 2004 route des Lucioles, Sophia Antipolis, France

C. Aldo Rinaldi is with the Department of Cardiology, Guy's and St Thomas' NHS Foundation Trust, St Thomas' Hospital, London, SE1 7EH, U.K.

Pier Lambiase is with the Heart Hospital, University College London Hospitals NHS Foundation Trust, London, NW1 2PG, U.K.

Maxime Sermesant is with the Asclepios project, INRIA, 2004 route des Lucioles, Sophia Antipolis, France and the Interdisciplinary Medical Imaging Group, Division of Imaging Sciences, King's College London, 4th Floor Lambeth Wing, St Thomas' Hospital, London, SE1 7EH, U.K.

- Biophysical models: semi-linear evolution Partial Differential Equation (PDE) with ionic models (up to fifty equations for ions and channels [4])
- Phenomenological models: semi-linear evolution PDE with mathematical simplification of biophysical models (bidomain, monodomain [5])
- Eikonal models: one static non-linear PDE for the depolarisation time derived from the previous models (eikonal curvature [6], eikonal diffusion (ED) [7])

Solutions of the evolution PDE are computationally very demanding, due to the space scale of the electrical propagation front being much smaller than the size of the ventricles. The motion of the front governed by the eikonal equation however is observed at a much larger scale, resulting in faster computations.

The inverse parameter estimation problem for cardiac electrophysiology models was previously attempted using ionic models [8], phenomenological models [9], and eikonal models [10]. However, as inverse problem solution techniques require multiple forward model evaluations, eikonal models are perhaps best suited with low forward model computational cost and less number of parameters to adjust. Further, meaningful clinical data currently available reliably describe the propagation times, but are not suited for accurate estimation of extra/intra cellular action potentials. For these reasons we chose to base our work with eikonal models as the forward model.

The paper is organised as follows. In section II, an adaptive zonal decomposition algorithm is presented for estimating volumetric apparent conductivity parameter from depolarisation isochronal measurements and a fast eikonal-diffusion electrophysiology model. Section III gives details of clinical data acquisition and presents the validation of the conductivity estimation algorithm with patient data, and followed by a brief discussion. Finally, conclusions are made and some future directions to improve the presented algorithm are indicated in section IV.

II. APPARENT CONDUCTIVITY ESTIMATION

In this section, we begin by explaining the forward electrophysiology model and then the adaptive zonal decomposition approach is outlined to estimate the apparent conductivity (AC). The definition of AC and its relation to tissue specific electrical conductivity is provided further in this section.

A. Forward Problem: Eikonal Diffusion Model

The static ED equation for the depolarisation time ($T(\mathbf{x})$) in the myocardium is given by

$$c_0 \sqrt{D(\mathbf{x})} \left(\sqrt{\nabla T(\mathbf{x})^t \mathbf{M} \nabla T(\mathbf{x})} \right) - \nabla \cdot (D(\mathbf{x}) \mathbf{M} \nabla T(\mathbf{x})) = \tau(\mathbf{x}), \tag{1}$$

where the superscript t denotes transpose, c_0 is a dimensionless constant related to the cell membrane and $\tau(\mathbf{x})$ is the cell membrane time constant. The tensor quantity relating to the fibre directions is given by $\mathbf{M} = \mathbf{A}\bar{\mathbf{D}}\mathbf{A}^t$, where $\mathbf{A}$ is the matrix defining the fibre directions in the global coordinate system and $\bar{\mathbf{D}} = \text{diag}(1, \lambda^2, \lambda^2)$. λ is the anisotropic ratio of space constants transverse and along the fibre direction and is set at 0.25 in the present paper. Other parameter values that are set are $c_0 = 2.5$ and $\tau = 0.79$ ms.

The nonlinear Equation (1) is solved using a fixed point iterative method combined with a very fast eikonal solver based on a modified anisotropic fast marching method (FMM) [11]. The FMM is a single-pass algorithm to solve the classical eikonal equation (without the diffusion term $\nabla \cdot (D\mathbf{M}\nabla T)$) and an anisotropic version presented earlier in [10] was extended to solve on volumetric unstructured mesh with tetrahedral elements.

As the method is based on fast marching which is an $\mathcal{O}(N \log(N))$ algorithm, where N denotes the number of nodes in the mesh, the electrical propagation is solved at a much faster rate as compared to the bi-domain or mono-domain equation based finite element models. For example, the solution of a 10000 node mesh can be achieved in the order of a few seconds, and hence the method is suitable for fast forward evaluations required in the inverse approach.

B. Adaptive zonal estimation algorithm

The adaptive algorithm is now outlined which enables the personalisation of the electrophysiology eikonal model from measured depolarisation times on the endocardial surface. The diffusion coefficient D in the ED equation is an intrinsic property of the myocardial tissue given by $D = \lambda_f^2 = \sigma_f \bar{r}_m$, where λ_f is the space constant in millimetres along the fibre direction, σ_f is the inverse of the sum of effective resistivities of intra and extra cellular domains and $\bar{r}_m$ is the inverse of membrane conductance per unit area. In this paper, we refer to the square root of the diffusion coefficient $\sqrt{D}$ as AC (d) in this paper and outline an algorithm to estimate this parameter. The AC value provides an indication of the extent of influence of the excitation wavefront at a particular point along the fibre direction [12].

The AC estimation algorithm is divided into two stages namely global and local. A nominal value of the AC d_{global} is first sought which minimises the mean error between the measured and simulated isochrones of depolarisation. This global estimation step enables us to bring the simulated isochrones using the model to the scale of measured isochrones and also provides us with a good initial estimate of AC for the local parameter estimation.

Once the simulated depolarisation time map globally fits the measured one, a local adjustment of the model is

possible. We begin by dividing the entire cardiac tissue Ω into prespecified M regions $R = \{\Omega_1, \Omega_2, \cdots, \Omega_M\}$. The conductivity is then assumed to be given by

$$d(\mathbf{x}) = \sum_{j=1}^{M} d_j \phi_j(\mathbf{x}), \tag{2}$$

where $\phi_j(\mathbf{x})$ is the Lagrange basis function defined on Ω_j. Thus the dimension of the problem is reduced to M. The AC values are obtained by minimising the discrete cost function given by

$$\mathscr{C}(\mathbf{d}) = \frac{1}{\mathscr{N}(\nu)} \sum_{v \in \nu} \left[T_v^m - T_v^s(d_{\Omega_1}, d_{\Omega_2}, \cdots, d_{\Omega_M}) \right]^2, \tag{3}$$

where ν denotes the set of all the vertices of the endocardial surface and $\mathscr{N}(.)$ denotes the set's cardinality, T_v^m denotes the measured depolarisation time at the vertex v and $T_v^s(d_{\Omega_1}, d_{\Omega_2}, \cdots, d_{\Omega_M})$ denotes the depolarisation time obtained by solving the fast electrophysiological model with the AC values set as $\{d_{\Omega_j}\}_{j=1}^{M}$.

A multilevel approach is pursued to solve the estimation problem. We begin with a minimum number of subdivisions (zones) of the volume. At each level, an iterative approach is used to estimate the zonal conductivity values. At each iteration we estimate a conductivity value for each subregion. The M−dimensional minimisation problem is converted into a series of one dimensional minimisation problems by varying the AC value on one considered subregion and keeping all other subregion's AC constant. The order in which the subregions are considered for minimisation follows the causality of the electrical wave propagation. This is achieved by pre-ordering the M zones according to the mean measured depolarisation times of all the endocardial vertices present in each zone. The one dimensional minimisation is achieved using a modified Brent algorithm detailed in a previous publication [10]. After convergence, the zone with maximal difference between mean T^m and mean T^s is further subdivided and the algorithm proceeds to the next level.

III. APPLICATION TO PATIENT DATA

In this section, we present the application of the proposed AC estimation algorithm on patient data suffering from left bundle branch block. The patient was a 60 year old female with NYHA class III symptoms (NYHA classes stand for the stages of heart failure according to the New York Heart Association). The aetiology of heart failure is thought to be dilated cardiomyopathy although cardiac MRI did show two non-viable areas of a moderate size which are consistent with a previous subendocardial infarction. The clinical data acquisition and fusion procedure is briefly outlined and then description of electrophysiology model inputs (anatomy, fibres) is provided. We then apply the estimation algorithm for three different isochronal datasets obtained during baseline (sinus rhythm) and two endocardial pacing positions.

A. Clinical Data Acquisition and Fusion

The MR examination involved balanced SSFP Cine imaging for the estimation of ventricular geometry, function and

2908

volumes, and late enhancement images with gadolinium contrast agent for scar anatomy. The electrical data was obtained by performing non-contact mapping using the Ensite 3000 multi-electrode array catheter system (St Jude, Sylmar, CA). We use a real-time registration solution as described in [13] that allows the spatial integration of MRI-based anatomical and functional data with X-ray-based catheter data, such as intracardiac electrical and pressure signals.

B. Model Inputs Preparation

The electrophysiology model in section II requires patient-specific anatomy and a description of cardiac fibre orientation. Image processing tools have been utilised to extract the bi-ventricular myocardium from the patient's cine-MRI images. The workflow consisted of 1) image preparation, in order to enhance image quality; 2) interactive segmentation of the myocardial boundaries at mid diastole; and 3) construction of the volumetric anatomical model. For regional personalisation of the simulation, each tetrahedron is automatically labelled according to the anatomical region it belongs to (LV+septum, RV, scar tissue, see Fig 1). The scar label is based on the expert manual delineation on late enhancement MRI. The fibre description was obtained from the statistical atlas of the cardiac fibre architecture and methodology as described in [14] (see Fig. 1b).
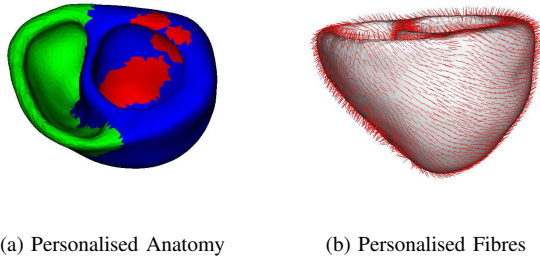

(a) Personalised Anatomy   (b) Personalised Fibres

Fig. 1. (a) 3D anatomical model of patient myocardium with anatomical labelling (LV in blue, RV in green and scar in red);(b) Personalised fibre orientations obtained from database

C. AC Estimation

In this section, we present the results obtained using the AC estimation algorithm adjusted with three different depolarisation isochrones sets. The three sets include the isochrones for normal sinus rhythm (baseline) and for two endocardial pacing locations i.e., P1 (apical) and P2 (septal-posterior). The biventricular myocardium was initially divided into a right ventricle (RV) and three left ventricular (LV) (septal-posterior, septal-anterior and lateral) subregions (see Fig 2a for labels and anterior direction is coming out of the page and posterior direction is into the page). As the depolarisation measurements were only on the LV endocardial surface, care was taken so as not to optimise in the regions where there were no endocardial nodes. The RV AC value was set to estimated d_{global} value. Note should be made of the way in which the subdivision at each level

was performed. The considered region was subdivided along the circumferential and long axis placed at the barycentre of the region. No division was performed in the wall thickness direction. Thus each considered region was divided into 4 segments with full wall thickness. The performance results are presented in Table I.

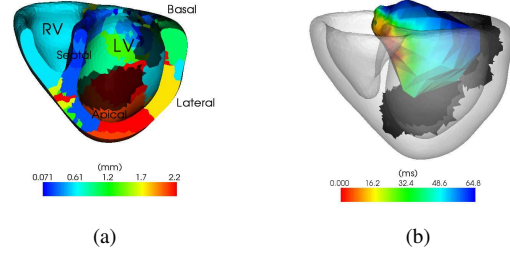(a)   (b)

Fig. 2. (a) Apparent conductivity map (units = mm) obtained from baseline isochrones. The bi-ventricular mesh was cut along a plane in the long axis direction. The black transparent regions show the scar locations and the blue colour in the septal region (low AC) clearly indicates the patient having left bundle branch block; (b) Ensite data (geometry and baseline isochrones) and MRI derived volumetric myocardial mesh in MR scanner coordinates. The isochronal data on the MR endocardial surface is obtained by nearest neighbour interpolation from the ensite geometry.

D. Results and Discussion

The apparent conductivity maps estimated for all three data sets are shown in Fig. 3 along with the scar locations obtained from late enhancement images (transparent black regions). From these figures, it can be seen that low apparent conductivity value (blue) regions do correspond with scar locations (Basal scar - all three subfigures and Apical scar - P2 pacing location). Further, as can be seen from Fig. 2a and Fig. 3, all the maps show a marked decrease in AC in the septal region. This is probably due to the left bundle branch block. Statistics are provided in Fig. 4.

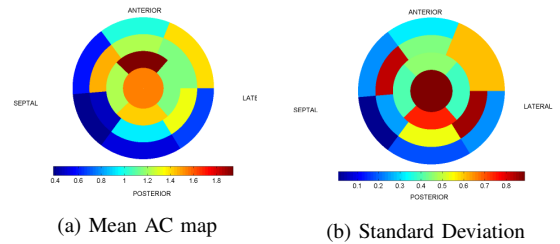(a) Mean AC map   (b) Standard Deviation

Fig. 4. (a) Mean and (b) Standard deviation of AC estimated for the patient displayed on the 17 segment AHA model bullseye plot

TABLE I
PERFORMANCE ESTIMATES OF THE AC ESTIMATION ALGORITHM

Mode	$\mathscr{C}(initial)$	$\mathscr{C}(global)$	d_{global}	$\mathscr{C}(final)$	M
Baseline	441.292	89.59	0.576	5.687	50
P1 (apical)	541.938	114.366	0.576	12.38	50
P2 (septal-posterior)	445.38	98.8134	0.576	12.02	37

2909

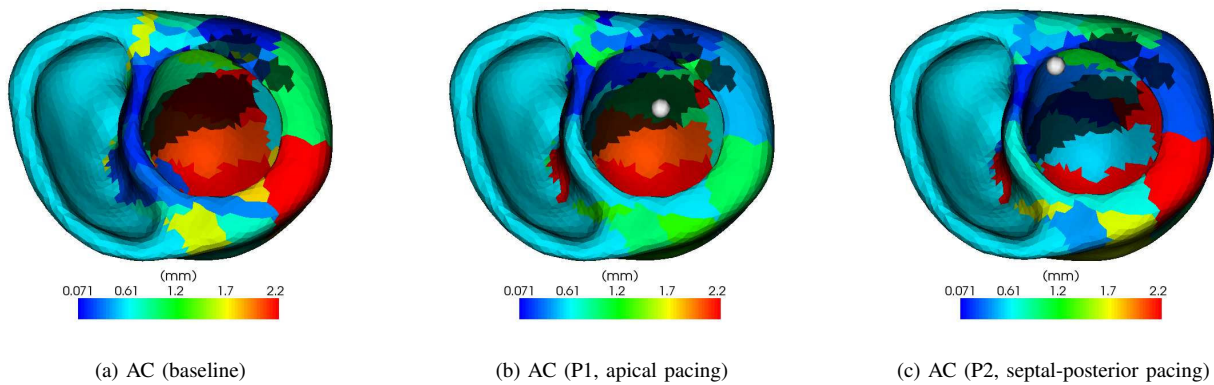(a) AC (baseline)   (b) AC (P1, apical pacing)   (c) AC (P2, septal-posterior pacing)

Fig. 3. Apparent conductivity maps (units = mm) estimated using ensite isochrones of depolarisation of (a) normal sinus rhythm (baseline); (b),(c) different endocardial pacings. The spheres represent the pacing catheter tip locations. The transparent black regions in all three figures indicate the scar location obtained from expert segmentation of late enhancement cardiac MRI images.The myocardium is viewed from the valve plane towards the apex.

In Fig. 3a and Fig. 3b, the estimation algorithm indicates high apparent conductivity in the region of the apical scar. This discrepancy can be explained by comparing the relative positions of endocardial surface generated with ensite during the electrophysiology measurement study and the actual MR derived biventricular myocardium (see Fig. 2b). The ensite balloon was much further from the apex location (≈ 50.89mm), thus decreasing the reliability of measured isochrones corresponding to the apical region. The limitations of the present study was that the method was evaluated in a single patient and incorporating more subjects is an ongoing piece of work.

IV. CONCLUSION

An adaptive zonal decomposition algorithm is presented to estimate volumetric apparent conductivity of myocardial tissue by solving an inverse problem. Such estimation algorithms pave the way towards personalisation of cardiac electrophysiological models. The algorithm obtains an estimate of the conductivity parameter by minimising the difference between simulated isochrones of an eikonal model to the measured isochrones of depolarisation. The algorithm has been applied on patient data obtained in a hybrid x-ray/magnetic resonance imaging environment. The conductivity maps obtained show a reasonable consistency even though the pacing locations were changed. Possible regions of slow conduction (low AC) have been identified and shown to correlate with scar locations obtained using late enhancement MR image segmentations using this procedure. The limitation of the present work is that the conductivity estimation is performed on the entire wall thickness and a topic of future work is to incorporate estimation even across the wall thickness. The accuracy of AC estimation could also be improved by incorporating epicardial depolarisation times measured by catheters in the coronary network.

V. ACKNOWLEDGMENTS

REFERENCES

[1] E. J. Crampin, M. Halstead, P. Hunter, P. Nielsen, D. Noble, N. Smith, and M. Tawhai, "Computational physiology and the physiome project," *Experimental Physiology*, vol. 89, no. 1, pp. 1–26, 2004.

[2] P. Hunter and P. Nielsen, "A strategy for integrative computational physiology," *Physiology (Bethesda)*, vol. 20, pp. 316–325, 2005.

[3] A. Hodgkin and A. Huxley, "A quantitative description of membrane current and its application to conduction and excitation in nerve," *J. of Physio.*, vol. 177, pp. 500–544, 1952.

[4] C. Luo and Y. Rudy, "A model of the ventricular cardiac action potential. depolarization, repolarization and their interaction," *Circ. Res.*, vol. 68, no. 6, pp. 1501–1526, 1991.

[5] A. Pollard, N. Hooke, and C. Henriquez, "Cardiac propagation simulation," *Crit. Rev. Biomed. Eng.*, vol. 20, no. 3-4, pp. 171–210, 1992.

[6] J. P. Keener, "An eikonal-curvature equation for action potential propagation in myocardium," *J. Math. Biol.*, vol. 29, pp. 629–651, 1991.

[7] P. C. Franzone, L. Guerri, and S. Rovida, "Wavefront propagation in activation model of the anisotropic cardiac tissue," *J. Math. Biol.*, vol. 28, no. 2, pp. 121–176, 1990.

[8] S. Dokos and N. H. Lovell, "Parameter estimation in cardiac ionic models," *Progress in Biophysics and Molecular Biology*, vol. 85, no. 2-3, pp. 407–431, 2004.

[9] M. Pop, M. Sermesant, D. Lepiller, M. V. Truong, E. R. McVeigh, E. Crystal, A. Dick, H. Delingette, N. Ayache, and G. A. Wright, "Fusion of optical imaging and mri for the evaluation and adjustment of macroscopic models of cardiac electrophysiology: A feasibility study," *Med. Image Anal.*, vol. 13, no. 2, pp. 370–380, 2009.

[10] P. Chinchapatnam, K. S. Rhode, M. Ginks, C. A. Rinaldi, P. Lambiase, R. Razavi, S. Arridge, and M. Sermesant, "Model-based imaging of cardiac apparent conductivity and local conduction velocity for diagnosis and planning of therapy," *IEEE Trans. Med. Imaging*, vol. 27, no. 11, pp. 1631–1642, 2008.

[11] M. Sermesant, E. Konukoglu, H. Delingette, Y. Coudiere, P. Chinchapatnam, K. S. Rhode, R. Razavi, and N. Ayache, "An anisotropic multi-front fast marching method for real-time simulation of cardiac electrophysiology," in *Functional Imaging and Modelling of the Heart*, 2007.

[12] K. A. Tomlinson, "Finite elements solution of eikonal equation for excitation wavefront propagation in ventricular myocardium," Ph.D. dissertation, The University of Auckland, New Zealand, 2000.

[13] K. S. Rhode, M. Sermesant, D. Brogan, S. Hegde, J. Hipwell, P. Lambiase, E. Rosenthal, C. Bucknall, S. A. Qureshi, J. S. Gill, R. Razavi, and D. L. G. Hill, "A system for real-time XMR guided cardiovascular intervention," *IEEE Trans. on Med. Imaging*, vol. 24, no. 11, pp. 1428–1440, 2005.

[14] J.-M. Peyrat, M. Sermesant, X. Pennec, H. Delingette, C. Xu, E. R. McVeigh, and N. Ayache, "A computational framework for the statistical analysis of cardiac diffusion tensors: application to small database of canine hearts," *IEEE Trans. on Med. Imaging*, vol. 26, no. 11, pp. 1500–1514, 2007.